

Density Functional Theory Study on the Mechanism of Rh-Catalyzed Decarboxylative Conjugate Addition: Diffusion- and Ligand-Controlled Selectivity toward Hydrolysis or β -Hydride Elimination

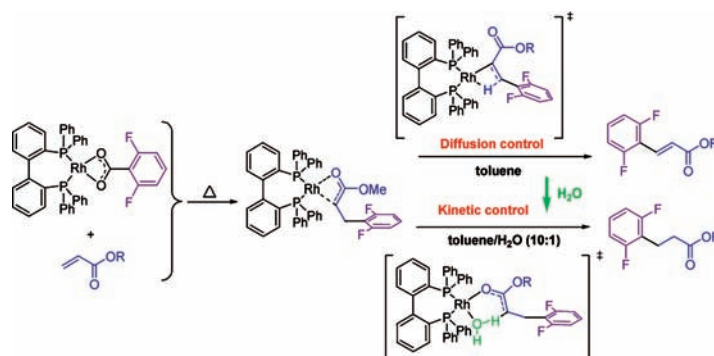
Fu-Qiang Shi*

Department of Chemistry, The University of Hong Kong, Pokfulam Road, Hong Kong, People's Republic of China

shifq@hku.hk

Received December 9, 2010

ABSTRACT



The mechanism of Rh-catalyzed decarboxylative conjugate addition has been investigated with Density Functional Theory (DFT). Calculations indicate that the selectivity toward hydrolysis or β -hydride elimination of the investigated reaction is a compromise between diffusion control and kinetic control. Ligand control can be adjusted by modifying the intermolecular interaction between the Rh(I) enolate intermediate and water.

Decarboxylative transformations of benzoic acids under the catalysis of late transition metals have attracted much interest in the past few years.¹ Decarboxylative coupling

utilizes readily available carboxylic acids as starting material, thus precluding the preparation of sensitive organometallic reagents. Cu and Pd have been widely used as catalysts for decarboxylation.²

(1) (a) Goossen, L. J.; Rodriguez, N.; Goossen, K. *Angew. Chem., Int. Ed.* **2008**, *47*, 3100. (b) Bonesi, S. M.; Fagnoni, M.; Albini, A. *Angew. Chem., Int. Ed.* **2008**, *47*, 10022.

(2) (a) Shepard, A. F.; Wilson, N. R.; Johnson, J. R. *J. Am. Chem. Soc.* **1930**, *52*, 2083. (b) Nilsson, M. *Acta Chem. Scand.* **1966**, *20*, 423. (c) Nilsson, M.; Ullenius, C. *Acta Chem. Scand.* **1968**, *22*, 1998. (d) Cairncross, A.; Roland, J. R.; Henderson, R. M.; Shepard, W. A. *J. Am. Chem. Soc.* **1970**, *92*, 3187. (e) Cohen, T.; Schambach, R. A. *J. Am. Chem. Soc.* **1970**, *92*, 3189. (f) Dickstein, J. S.; Mulrooney, C. A.; O'Brien, E. M.; Morgan, B. J.; Kozlowski, M. *Org. Lett.* **2007**, *9*, 2441.

(3) (a) Myers, A. G.; Tanaka, D.; Mannion, M. R. *J. Am. Chem. Soc.* **2002**, *124*, 11250. (b) Tanaka, D.; Myers, A. G. *Org. Lett.* **2004**, *6*, 433. (c) Maehara, A.; Tsurugi, H.; Satoh, T.; Miura, M. *Org. Lett.* **2008**, *10*, 1159. (d) Hu, P.; Kan, J.; Su, W.; Hong, M. *Org. Lett.* **2009**, *11*, 2341.

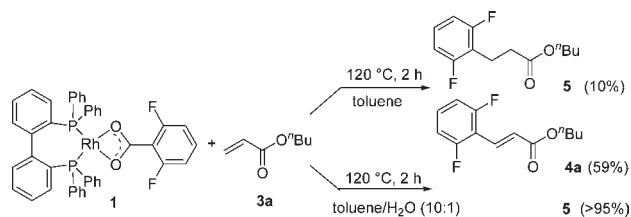
(4) (a) Goossen, L. J.; Deng, G.; Levy, L. M. *Science* **2006**, *313*, 662. (b) Goossen, L. J.; Rodriguez, N.; Melzer, B.; Linder, C.; Deng, G.; Levy, L. M. *J. Am. Chem. Soc.* **2007**, *29*, 4824. (c) Goossen, L. J.; Melzer, B. *J. Org. Chem.* **2007**, *72*, 7473. (d) Goossen, L. J.; Rudolphi, F.; Opper, C.; Rodriguez, N. *Angew. Chem., Int. Ed.* **2008**, *47*, 3043. (e) Goossen, L. J.; Zimmermann, B.; Knauber, T. *Angew. Chem., Int. Ed.* **2008**, *47*, 7103. (f) Goossen, L. J.; Manjolinho, F.; Khan, B. A.; Rodriguez, N. *J. Org. Chem.* **2009**, *74*, 2620. (g) Núñez Magro, A. A.; Eastham, G. R.; Cole-Hamilton, D. J. *Dalton Trans.* **2009**, 4683. (h) Goossen, L. J.; Linder, C.; Rodriguez, N.; Lange, P. P.; Fromm, A. *Chem. Commun.* **2009**, 7173. (i) Goossen, L. J.; Rodriguez, N.; Lange, P. P.; Linder, C. *Angew. Chem., Int. Ed.* **2010**, *49*, 1111.

In 2002, Myers et al.³ introduced a novel Heck reaction in which the aromatic carboxylic acids are treated with alkenes in the presence of silver carbonate and a palladium catalyst with the release of CO₂ to form vinyl arenes, which has inspired the expansion of this decarboxylation strategy for various catalytic reactions.^{4–8} Afterward, Myers et al.⁹ performed an experimental study on the mechanism of palladium-mediated decarboxylative olefination of arene carboxylic acids. The study shows that there are notable differences in reactivity between arylpalladium(II) intermediates generated by decarboxylative palladation and those produced in conventional Heck reactions. Namely, more electron-rich alkenes react preferentially with an arylpalladium(II) trifluoroacetate intermediate formed by decarboxylative palladation, whereas an opposite trend is found in conventional Heck reactions.

The systemic analysis of factors controlling Pd-catalyzed decarboxylative coupling was also conducted with Density Functional Theory (DFT).¹⁰ The catalytic cycle was found to comprise four steps: decarboxylation, olefin insertion, β -hydride elimination, and catalyst regeneration. Decarboxylation was the rate-limiting step, and it proceeded through a dissociative pathway in which Pd(II) mediated the extrusion of CO₂ from an aromatic carboxylic acid to form a Pd(II)–aryl intermediate.

Recently, Zhao et al.¹¹ developed the rhodium-catalyzed conjugate addition of fluorinated benzoic acids with an α,β -unsaturated carbonyl derivative (Scheme 1). The treatment of **1** with excess *n*-butyl acrylate (**3a**, 6 equiv) in dry toluene at 120 °C gave a mixture of the conjugate-addition product **5** and a Heck–Mizoroki product **4a** (1:6) in 69% combined yield. In contrast, when the reaction was carried out in a 10:1 mixture of toluene and H₂O, **5** was formed selectively in near-quantitative yield. However, even in the presence of water, very low selectivity (1.4:1) was observed when 1,4-bis(diphenylphosphanyl)butane (dppb) ligand was used.¹¹ Interestingly, the ligand (*R,R*)-DIOP

Scheme 1. Rh(I)-Catalyzed Conjugate Addition

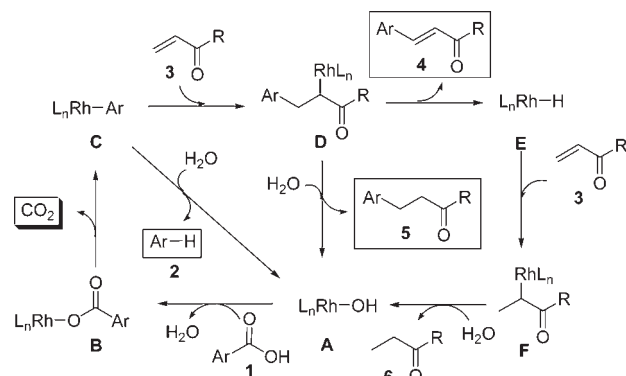


promoted the selective formation of **4a** over **5** in the presence of water.

The proposed mechanisms, which involve three potential catalytic cycles, are shown in Scheme 2.¹¹

Even though theoretical computations have already found that water can act as both a solvent and a catalyst in substituted benzoic acids decarboxylation,¹² to the best of our knowledge, no theoretical study on the mechanism of the rhodium-mediated decarboxylative conjugate addition in the absence/presence of water has been reported.

Scheme 2. Proposed Mechanism of Rh(I)-Catalyzed Decarboxylative Transformations



(5) (a) Forgiione, P.; Brochu, M.-C.; St-Onge, M.; Thesen, K. H.; Bailey, M. D.; Bilodeau, F. *J. Am. Chem. Soc.* **2006**, *128*, 11350. (b) Becht, J.-M.; Catala, C.; Le Drian, C.; Wagner, A. *Org. Lett.* **2007**, *9*, 1781. (c) Voutchkova, A.; Coplin, A.; Leadbeater, N. E.; Crabtree, R. H. *Chem. Commun.* **2008**, 6312. (d) Shang, R.; Fu, Y.; Wang, Y.; Xu, Q.; Yu, H.-Z.; Liu, L. *Angew. Chem., Int. Ed.* **2009**, *48*, 9350. (e) Cornella, J.; Lu, P.; Larrosa, I. *Org. Lett.* **2009**, *11*, 5506.

(6) (a) Cornella, J.; Sanchez, C.; Banawa, D.; Larrosa, I. *Chem. Commun.* **2009**, 7176. (b) Lu, P.; Sanchez, C.; Cornella, J.; Larrosa, I. *Org. Lett.* **2009**, *11*, 5710.

(7) (a) Rayabarapu, D. K.; Tunge, J. A. *J. Am. Chem. Soc.* **2005**, *127*, 13510. (b) Waetzig, S. R.; Rayabarapu, D. K.; Weaver, J. D.; Tunge, J. A. *Angew. Chem., Int. Ed.* **2006**, *45*, 4977. (c) Burger, E. C.; Tunge, J. A. *J. Am. Chem. Soc.* **2006**, *128*, 10002. (d) Waetzig, S. R.; Tunge, J. A. *J. Am. Chem. Soc.* **2007**, *129*, 4138. (e) Waetzig, S. R.; Tunge, J. A. *J. Am. Chem. Soc.* **2007**, *129*, 14860. (f) Weaver, J. D.; Tunge, J. A. *Org. Lett.* **2008**, *10*, 4657.

(8) (a) Ueura, K.; Satoh, T.; Miura, M. *J. Org. Chem.* **2007**, *72*, 5362. (b) Shimizu, M.; Hirano, K.; Satoh, T.; Miura, M. *J. Org. Chem.* **2009**, *74*, 3478.

(9) Tanaka, D.; Romeril, S. P.; Myers, A. G. *J. Am. Chem. Soc.* **2005**, *127*, 10323.

(10) (a) Shang, R.; Fu, Y.; Li, J.-B.; Zhang, S.-L.; Guo, Q.-X.; Liu, L. *J. Am. Chem. Soc.* **2009**, *131*, 5738. (b) Zhang, S.-L.; Fu, Y.; Shang, R.; Guo, Q.-X.; Liu, L. *J. Am. Chem. Soc.* **2010**, *132*, 638. (c) Shang, R.; Xu, Q.; Jiang, Y.-Y.; Wang, Y.; Liu, L. *Org. Lett.* **2010**, *12*, 1000.

(11) (a) Sun, Z.-M.; Zhao, P. *Angew. Chem., Int. Ed.* **2009**, *48*, 6726. (b) Sun, Z.-M.; Zhang, J.; Zhao, P. *Org. Lett.* **2010**, *12*, 992.

(12) (a) Chuchev, K.; BelBruno, J. J. *THEOCHEM* **2007**, 807, 1. (b) Li, J.; Brill, T. B. *J. Phys. Chem. A* **2003**, *107*, 2667.

(13) Shi, F.-Q.; Li, X.; Xia, Y.; Zhang, L.; Yu, Z.-X. *J. Am. Chem. Soc.* **2007**, *129*, 15503.

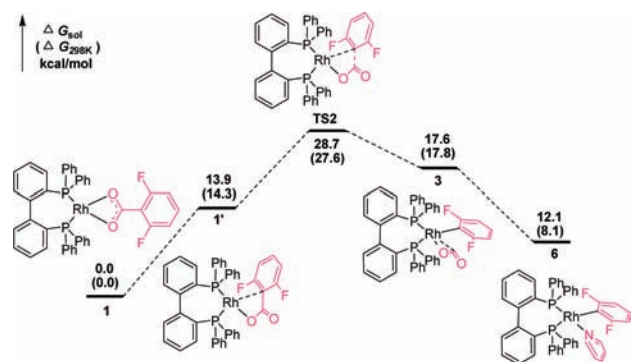


Figure 1. DFT computed free energy profile of Rh(I)-catalyzed decarboxylation.

Rh–O bonds and C–O bond in optimized **1** are slightly longer than those in the solid state, which may due to the crystal packing. Intermediate **1** first isomerizes to **1'**, which is less stable than **1** by 13.9 kcal/mol in toluene (14.3 kcal/mol in gas phase) (Figure 1). In the calculated four-membered ring decarboxylation transition state **TS2**, both CO₂ and a phenyl anion coordinate to [(biphep)Rh]⁺ through the lone pair of carbon and oxygen, respectively. The C1–C2 distance in **TS2** is 2.080 Å, which shows the C1–C2 has been partly broken (its Wiberg bond indices is 0.35).

The activation free energy (28.7 kcal/mol) is consistent with the experimental temperature required for the reaction (120 °C). The decarboxylation process is a strongly endothermic process (17.6 kcal/mol). This energetically disfavored reaction should be promoted by decreasing the concentration of decarboxylative products. This may explain why the choice of NaOH as an inorganic additive was also critical for satisfactory results in the title reaction, in which NaOH may act as a CO₂ scavenger to promote decarboxylation.^{11,14} Pyridine can complex with the intermediate generated from **3** by releasing CO₂. In the presence of methyl acrylate, the decarboxylation product **3** can convert to **4** via a ligand exchange process, in which CO₂ is substituted for methyl acrylate. Intermediate **4** can undergo migratory insertion with added methyl acrylate, forming a new C–C bond in a Rh(I) enolato intermediate **7** (Figure 2). The insertion step requires an activation free energy of 19.0 kcal/mol. The η³-complex **7** is more stable than **4** by 18.9 kcal/mol.

For β-hydride elimination, intermediate **7** must overcome an energy barrier of 9.1 kcal/mol to give the energetically disfavored isomer **8**. The basis for **7** being more stable than **8** is because the C3–C4 and Rh–H bonds in **8** have achieved a nearly coplanar geometry for β-hydride elimination, which results in more steric repulsion. β-Hydride elimination of **8** leads to **10** via **TS9**. In contrast, in the presence of water, **7** and water can form a complex **7-H₂O**, and this complexation process is endergonic by 9.8 kcal/mol. Then, hydrogen transfer of **7-H₂O** generates **12**

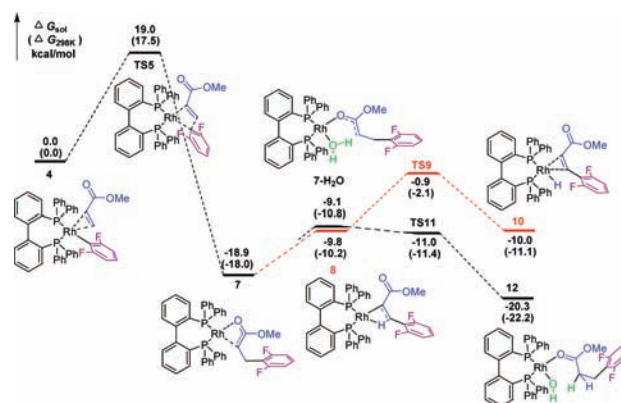


Figure 2. DFT computed free energy profile for the Rh(I)-catalyzed conjugate addition.

via **TS11**. **TS11** is slightly more stable than **7-H₂O** by 1.9 kcal/mol; therefore, this hydrogen transfer step is barrierless.

The β-hydride elimination requires an activation free energy of 18.0 kcal/mol (Figure 2). In contrast, only 9.8 kcal/mol is required to overcome the barrier of complexation between **7** and water. If only comparing the stabilities of **TS9** and **TS11**, **5** should be formed selectively in quantitative yield. This is not in agreement with the aforementioned experimental results (59% **4a** and 10% **5**). It should be noted that the transformation from **7** to **7-H₂O** is an intermolecular process; in contrast, the transformation from **7** to **8** is an intramolecular process. It is known that the intramolecular transformation is expected to be faster than the intermolecular complexation. Based on the experimental result, it can be concluded that there is a thermodynamic equilibrium between **7** and **8**. Though **7** is more stable than **8** (9.1 kcal/mol), the minor isomer **8** reacts much faster than the complexation between **7** and water. That is to say, under title reaction conditions (120 °C), a vast majority of intermediate **7** can easily transform to **4a** via β-hydride elimination before complexation with water occurs, because only tiny amount of water exists in the reaction system. Therefore, the ratio of **4a** to **5** is diffusion controlled by the energy difference between **TS9** and **7-H₂O**.

To further verify this hypothesis, we investigated the [(dppb)Rh(I)]⁺ catalyzed cycle. Calculations indicate that the energy difference between **TS9** and **7-H₂O** decreases from 8.2 to 1.8 kcal/mol when the biphep ligand is displaced by the dppb ligand, which is consistent with the decreasing selectivity (from 99:1 to 1.4:1). This shows that the selectivity toward hydrolysis or β-hydride elimination of the investigated reaction is a compromise between diffusion control and kinetic control.

However, when water was added as cosolvent, the intermediate **7** will easily complex with water. By now, kinetic control dominates diffusion control. This can well explain why **5** is formed selectively in near-quantitative yield in a 10:1 mixture of toluene and H₂O.

(14) Goossen, L. J.; Rodríguez, N.; Linder, C. J. *Am. Chem. Soc.* **2008**, *130*, 15248.

Calculations indicate that Heck–Mizoroki olefination is a very easy process, which only requires activation free energy of 10.6 kcal/mol (Figure S1 in the Supporting Information). So excess olefin should be required to act as a sacrificial hydrogen acceptor, which is confirmed by experimental observation.

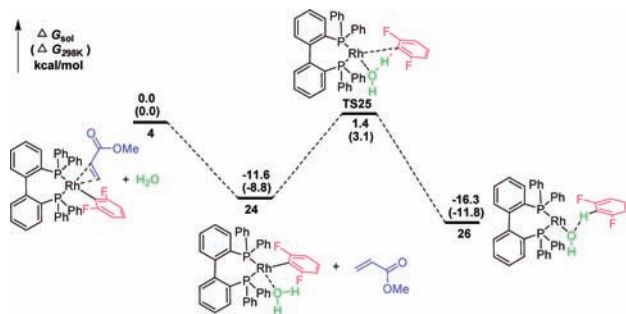


Figure 3. DFT computed free energy profile for the Rh(I)-catalyzed hydrodecarboxylation.

Intermediate **4** can also lead to **24** via a ligand exchange process, which is exothermic by 11.6 kcal/mol (Figure 3). A hydrogen shift through **TS25** leads to the formation of **26**. The hydrogen shift step is exergonic by 4.7 kcal/mol and requires an activation free energy of 13.0 kcal/mol, which indicates that the arene product can be readily obtained after decarboxylation. The activation free energy of the reverse reaction is 14.9 kcal/mol, which indicates the hydrogen shift step is reversible.

To investigate the origin of the selective formation of **4a** over **5** in the presence of (*R,R*)-DIOP, we calculated the [(*R,R*)-DIOPRh(I)]⁺ catalyzed cycle (Figure 4). It is noteworthy that the complexation between the Rh(I) enolato intermediate and H₂O become more disfavored when the biphep ligand is displaced by the (*R,R*)-DIOP ligand (9.1 vs 10.8 kcal/mol). This causes the precursor of hydrolysis, **18-H₂O**, to be less stable than that of β -hydride elimination, **19**, by 3.5 kcal/mol. At the same time, the activation free energy of β -hydride elimination decreases from 18.0 to 15.7 kcal/mol. Decreasing activation free energy and increasing complexation energy result in β -hydride elimination becoming easier and hydrolysis becoming more difficult. The net result is that the ratio of **4a**:**5** is reversed

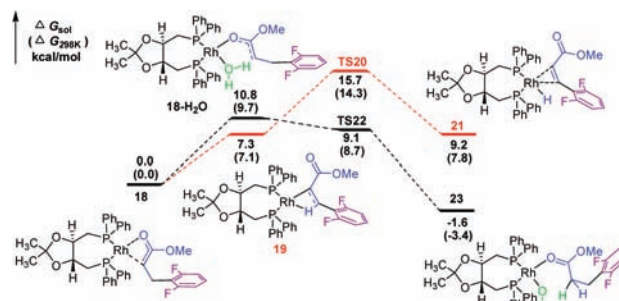


Figure 4. DFT computed free energy profile for the Rh(I)-catalyzed conjugate addition.

(19:1). The energy difference between **18-H₂O-F3/F5** and **TS20-F3/F5** is also calculated. It is found that more F substituents will increase the energy difference. Therefore, more F substituents are expected to decrease the ratio of **4a**:**5**, which is in agreement with the experiments (19:1 > 10:1 > 2:1).

In summary, the mechanism of the Rh-catalyzed decarboxylative conjugate addition of fluorinated benzoic acids has been computationally addressed using Density Functional Theory (B3LYP/6-31G*, LANL2DZ for Rh). Two competing reaction pathways (hydrolysis and β -hydride elimination) are investigated. Calculations reveal that diffusion control dominates when dry toluene is used. In contrast, when H₂O was added as cosolvent, kinetic control becomes dominant. It is also found that the intermolecular interaction between the Rh(I) enolato intermediate and H₂O plays an important role in affecting the balance between diffusion control and kinetic control. These results may have valuable implications for the design of a new, more effective catalytic system for decarboxylative couplings.

Acknowledgment. This study was supported by grants from NSFC (No. 20802011) and the author acknowledges Prof. Pinjing Zhao of North Dakota State University for his insightful suggestions.

Supporting Information Available. Optimized geometries and Cartesian coordinates of all computed species. This material is available free of charge via the Internet at <http://pubs.acs.org>.